

# **Omega 3 fatty acids attenuate the AKI to CKD transition and renal fibrosis: identification of antifibrotic metabolites**

Kai Tokumaru<sup>1</sup>, Tadashi Imafuku<sup>2</sup>, Takao Satoh<sup>3</sup>, Tomoaki Inazumi<sup>4</sup>, Shu Hirashima<sup>2</sup>, Ayano Nishinoiri<sup>1</sup>, Taisei Nagasaki<sup>2</sup>, Hitoshi Maeda<sup>2</sup>, Yukihiko Sugimoto<sup>4</sup>, Motoko Tanaka<sup>5</sup>, Kazutaka Matsushita<sup>5</sup>, Toru Maruyama<sup>2</sup>, Hiroshi Watanabe<sup>1</sup>

<sup>1</sup>Department of Clinical Pharmacy and Therapeutics, Graduate School of Pharmaceutical Sciences, Kumamoto University, Kumamoto, Japan

<sup>2</sup>Department of Biopharmaceutics, Graduate School of Pharmaceutical Sciences, Kumamoto University, Kumamoto, Japan

<sup>3</sup>Kumamoto Industrial Research Institute, Kumamoto, Japan

<sup>4</sup>Department of Pharmaceutical Biochemistry, Graduate School of Pharmaceutical Sciences, Kumamoto University, Kumamoto, Japan

<sup>5</sup>Department of Nephrology, Akebono Clinic, Kumamoto, Japan

## **Supplemental Materials**

## Supplemental Methods

### Animal Experiments

The study was carried out in compliance with the ARRIVE guidelines. The animal care and use committee of Kumamoto University approved the protocols for all animal experiments (A2023-018). ICR mice (male, 21-day old; Japan SLC, Inc., Shizuoka, Japan) were maintained under controlled temperature conditions (21-23°C) with a 12 h light and 12 h dark cycle (light 8 am-8 pm). The mice were fed experimental diets for 4 weeks, supplemented with either 4% soybean or linseed oil (Oriental Yeast, Tokyo, Japan).<sup>1,2</sup> AKI, the AKI to CKD transition and UUO mice were induced as described previously.<sup>3,4</sup> Mice were allowed free access to water throughout the test period. AKI or the AKI to CKD transition were induced as described previously.<sup>3</sup> In brief, AKI or the AKI to CKD transition was induced by clamping renal pedicles for 35 min or 30 min, respectively at 37°C. To induce UUO, the left ureter was ligated with 4-0 silk, and the abdomen was closed with sutures. Following surgery, the mice were warmed at 37°C during the recovery period.<sup>4</sup>

### Measurement of fatty acids by gas chromatography-mass spectrometry (GC-MS)

Fatty acids in the kidney were extracted and analyzed as described previously.<sup>5</sup> In brief, samples of freeze-dried kidney tissue (50 mg) were mixed with chloroform (1 mL) and incubated at 50°C for 30 min. Extracts were clarified by centrifugation and then evaporated. Fatty acids derived from total lipids were methylated using a fatty acid methylation kit (Nacalai Tesque, Kyoto, Japan). Analysis by GC-MS (5975C inert XL MSD fitted with a capillary column 0.25 µm×30 m×0.25 mm, VF-WAXms; Agilent) allowed identification of the fatty acids. Nonadecanoic acid (Sigma-Aldrich, St. Louis, MO) was used as internal standard.

### **Measurement of polyunsaturated fatty acids (PUFAs) and their metabolites**

Lipid extraction and quantitative analysis of lipids using liquid chromatography-mass spectrometry (LC-MS) was performed as described previously.<sup>1</sup> Kidney tissues were homogenized in acetonitrile using a bead homogenizer. Prostaglandin (PG) E<sub>2</sub>-d4 (Cayman Chemical, Ann Arbor, MI) was used as internal standard. The supernatant was collected, and the sample acidified (pH 3 to 4) with HCl. Lipids were then purified using Oasis hydrophilic lipophilic balance extraction cartridges (Waters, Milford, MA). HPLC-negative-ion electrospray ionization-MS/MS analyses were performed using a Nexera X2 HPLC instrument (Shimadzu, Kyoto, Japan) and a triple quadrupole mass spectrometer QTRAP 5500 (SCIEX, Framingham, MA). A reverse-phase column (Kinetex C18, 1.7  $\mu$ m, 150 mm  $\times$  2.1 mm; Phenomenex, Torrance, CA) was used for chromatographic separation.

### **Cell culture**

Rat renal fibroblast cells (NRK-49F cells) were purchased from the RIKEN bioresource cell bank (Ibaraki, Japan). The culture medium of NRK-49F cells was prepared by adding 10% deactivated fetal bovine serum (Capricorn Scientific, Ebsdorfergrund, Germany), and an antibiotic/antimycotic mixture (penicillin (100 U/mL), streptomycin (100  $\mu$ g/mL), amphotericin B (0.25  $\mu$ g/mL)) to DMEM/Ham's F-12.

### **Evaluation of the antifibrotic effect using NRK-49F cells**

NRK49F cells were seeded on 6-well plates and cultured in a CO<sub>2</sub> incubator for 24 h at 37°C in 1% FBS. After washing with PBS, EPA, 18-HEPE, 17,18-EpETE, 17,18-diHETE (100 nM) was added and the cells were incubated for 12 h. TGF- $\beta$ 1 (Peprotech, NJ, USA) was then added to a final concentration of 10 ng/mL and the cells were incubated for a further 6 h before evaluation.

### **Effect of inhibiting Cyp on the biological activity of EPA**

The identification of fatty acid active metabolites by inhibition of metabolic enzymes was described in a previous report.<sup>6</sup> NRK-49F cells were seeded on 6-well plates and cultured in a CO<sub>2</sub> incubator for 24 h at 37°C in 1% FBS. After washing with PBS, the cells were incubated with 1-ABT (2.5 μM) for 30 min before adding EPA (50 μM). Cells were then incubated for a further 12 h. TGF-β1 was subsequently added to a final concentration of 10 ng/ml and the cells incubated for 6 h prior to evaluation.

### **Quantitative RT-PCR**

Total RNA from kidney tissue or cells was isolated and quantitative RT-PCR measurements performed as described previously.<sup>5</sup> The sequences of primers used for mRNA detection are shown in Supplemental Table 1. The threshold cycle (C<sub>t</sub>) values for each gene were normalized by subtracting the C<sub>t</sub> value calculated for glyceraldehyde-3-phosphate dehydrogenase.

### **Western blotting**

Western blotting analyses were performed as previously described.<sup>3</sup> Total protein was extracted with lysis buffer containing 50 mM Tris-HCl buffer (pH 6.8), 150 mM NaCl, 1% v/v NP-40 and 1% protease inhibitor cocktail (Nacalai Tesque, Kyoto, Japan). After centrifugation, the supernatant was mixed with reducing sample buffer and boiled for 3 min. Samples were resolved by 10% sodium dodecyl sulfate-polyacrylamide gel electrophoresis. The proteins were electroblotted onto a polyvinylidene fluoride membrane and subsequently subjected to immunoblotting using specific antibodies against α-SMA (ab569; Abcam, Cambridge, UK) at 4°C overnight. The membrane was then washed and probed with horseradish peroxidase-conjugated secondary antibody at room temperature for 1 h. Cross-reacting bands were detected using the LAS4000mini gel imaging system (GE Healthcare, Amersham, UK) and quantified with ImageJ

software. The densitometric intensity was normalized to  $\beta$ -actin expression. These antibodies are shown in Supplemental Table 2.

### **Histological examination of kidney tissues**

Harvested kidney tissues were fixed in 10% formalin neutral buffer solution for 48 h and then embedded in paraffin. Kidney blocks were cut into 2- $\mu$ m sections prior to performing staining procedures. Morphological analysis was carried out by periodic acid-Schiff (PAS) staining. The percentages of tubules that displayed cellular necrosis, loss of brush border, cast formation, vacuolization, and tubule dilation per 10 low-power fields (x200) were scored by 3 pathologists in a blind fashion, scale from 0 to 5 (0, none; 1, <10% 2, 11-25% 3, 26-45% 4, 46-75% and 5, >76%). Fibrosis was assessed after staining with Picosirius red. Immunohistostaining of  $\alpha$ -SMA was used as a myofibroblast marker. Images and quantification analyses were performed using a Keyence BZ-X710 microscope (Keyence, Osaka, Japan). Detailed procedures have been published elsewhere.<sup>3</sup>

### **Metabolomic Analysis**

Metabolomic analysis was performed using MetaboAnalyst 5.0 (<http://www.metaboanalyst.ca>). As a pre-processing step, missing values were imputed with 1/2 of the minimum value, and the data were log-transformed and autoscaled. For the volcano plot, the difference between the two groups was considered significant when the change was more than 2-fold and  $p<0.05$ .

### **Statistical Analyses**

The means for two-group data were compared by the unpaired t test. The means for groups were compared by ANOVA using the Tukey multiple comparison method (GraphPad Prism 9; San Diego, CA). Survival curves were constructed according to the Kaplan-Meier method (GraphPad

Prism 9; San Diego, CA). The Gehan-Breslow-Wilcoxon test was used to evaluate survival rate.

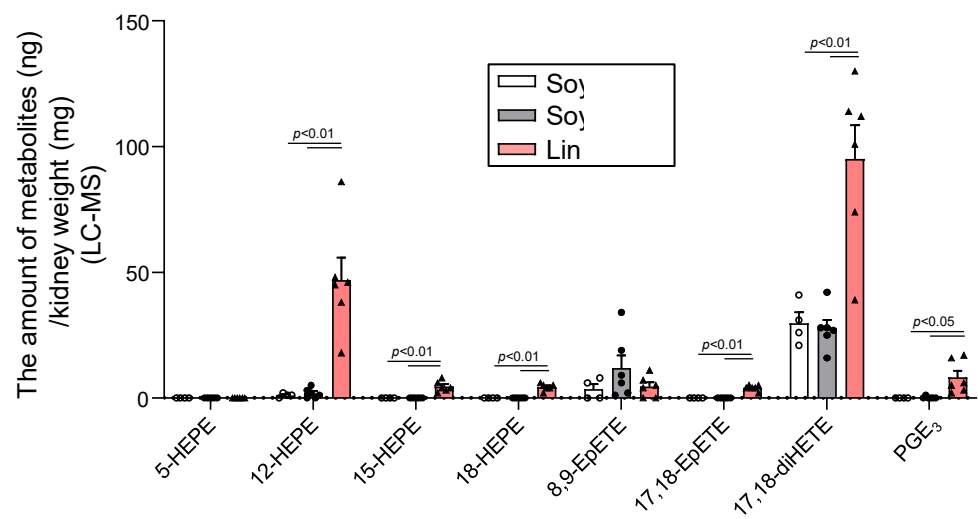
A probability value of  $p < 0.05$  was considered to be significant.

## References

1. Hashimoto M, Makino N, Inazumi T, Yoshida R, Sugimoto T, Tsuchiya S, Sugimoto Y: Effects of an  $\omega$ 3 fatty acid-biased diet on luteolysis, parturition, and uterine prostanoid synthesis in pregnant mice. *Biochem Biophys Res Commun* Jan 22 2022;589:139-146. doi:10.1016/j.bbrc.2021.12.029
2. Kunisawa J, Arita M, Hayasaka T, Harada T, Iwamoto R, Nagasawa R, Shikata S, Nagatake T, Suzuki H, Hashimoto E, Kurashima Y, Suzuki Y, Arai H, Setou M, Kiyono H: Dietary  $\omega$ 3 fatty acid exerts anti-allergic effect through the conversion to 17,18-epoxyeicosatetraenoic acid in the gut. *Sci Rep* Jun 11 2015;5:9750. doi:10.1038/srep09750
3. Nishida K, Watanabe H, Murata R, Tokumaru K, Fujimura R, Oshiro S, Nagasaki T, Miyahisa M, Hiramoto Y, Nosaki H, Imafuku T, Maeda H, Fukagawa M, Maruyama T: Recombinant Long-Acting Thioredoxin Ameliorates AKI to CKD Transition via Modulating Renal Oxidative Stress and Inflammation. *Int J Mol Sci* May 25 2021;22(11)doi:10.3390/ijms22115600
4. Bi J, Watanabe H, Fujimura R, Nishida K, Nakamura R, Oshiro S, Imafuku T, Komori H, Miyahisa M, Tanaka M, Matsushita K, Maruyama T: A downstream molecule of 1,25-dihydroxyvitamin D3, alpha-1-acid glycoprotein, protects against mouse model of renal fibrosis. *Sci Rep* Nov 26 2018;8(1):17329. doi:10.1038/s41598-018-35339-x
5. Imafuku T, Watanabe H, Satoh T, Matsuzaka T, Inazumi T, Kato H, Tanaka S, Nakamura Y, Nakano T, Tokumaru K, Maeda H, Mukunoki A, Takeo T, Nakagata N, Tanaka M, Matsushita K, Tsuchiya S, Sugimoto Y, Shimano H, Fukagawa M, Maruyama T: Advanced Oxidation Protein Products Contribute to Renal Tubulopathy via Perturbation of Renal Fatty Acids. *Kidney360* Aug 27 2020;1(8):781-796. doi:10.34067/kid.0000772019
6. Liu Y, Fang X, Zhang X, Huang J, He J, Peng L, Ye C, Wang Y, Xue F, Ai D, Li D, Zhu Y: Metabolic profiling of murine plasma reveals eicosapentaenoic acid metabolites protecting against endothelial activation and atherosclerosis. *Br J Pharmacol* Apr 2018;175(8):1190-1204. doi:10.1111/bph.13971

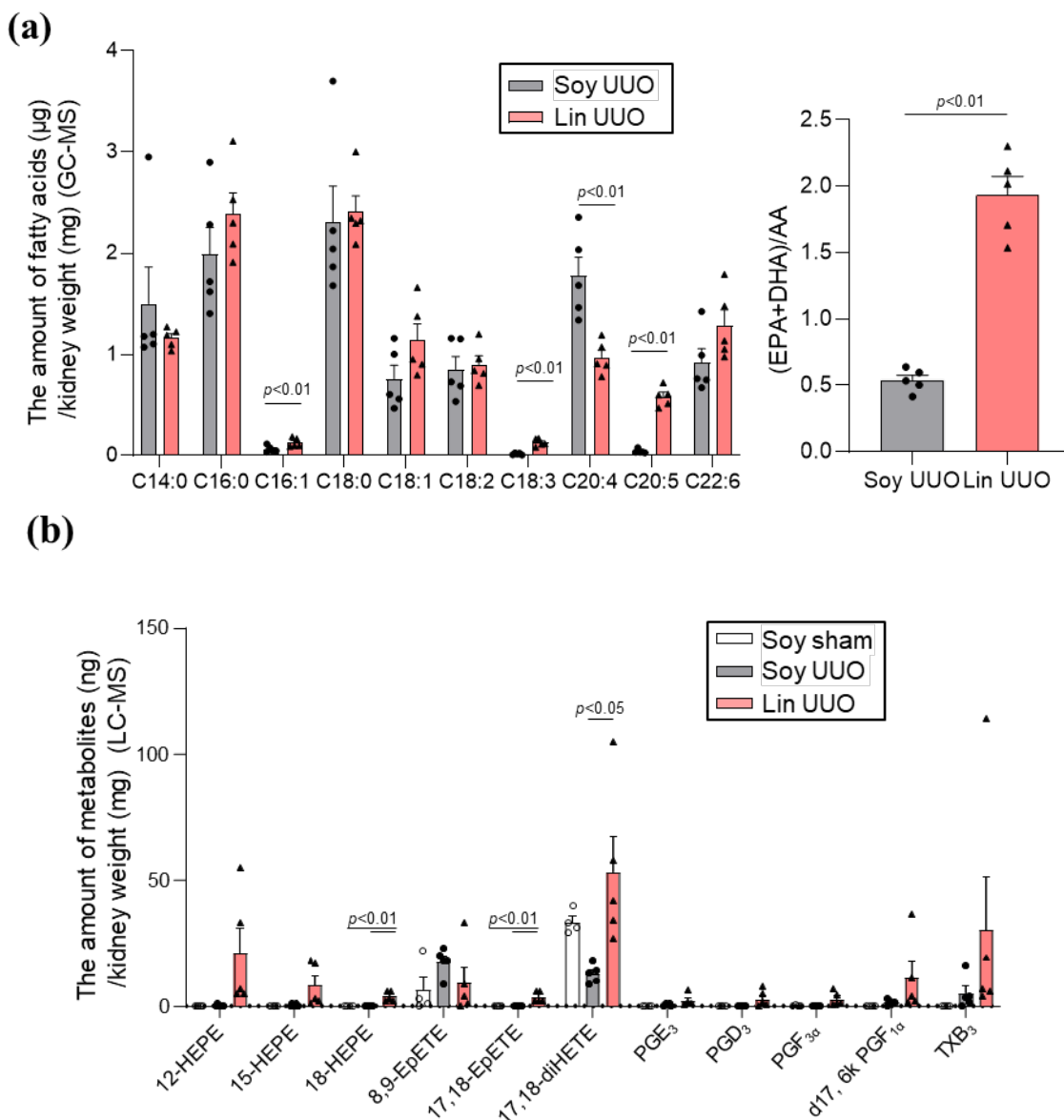
## Supplemental Figure 1

**Figure S1.** Effect of dietary soybean oil diet (Soy) or linseed oil diet (Lin) on eicosapentaenoic acid (EPA) metabolite levels in kidney tissues from renal IR mice. Data are expressed as means $\pm$ SE (n = 4-6).



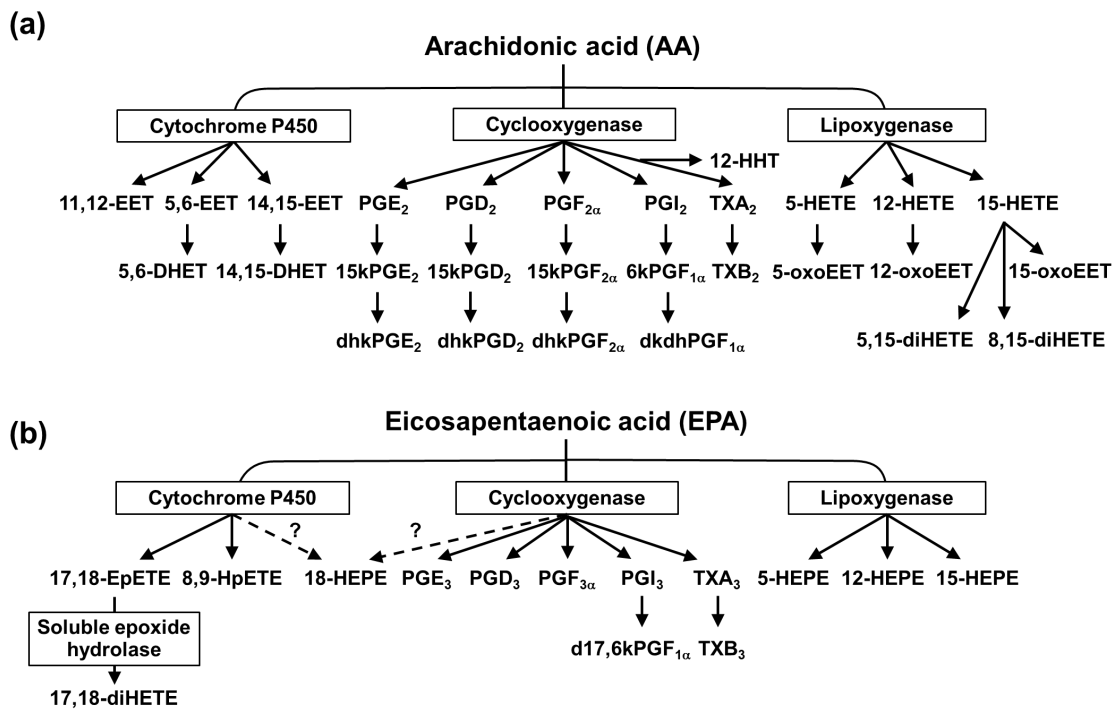
## Supplemental Figure 2

**Figure S2.** Effect of soybean oil diet (Soy) or linseed oil diet (Lin) on total free fatty acids and eicosapentaenoic acid (EPA) metabolites in the kidney of unilateral ureteral obstruction (UUO) mice. (a) Renal total fatty acid profiles were determined 7 days after UUO by GC-MS. The renal ((EPA)+docosahexaenoic acid (DHA))/arachidonic acid (AA) ratios were determined by GC-MS (n=5). (b) EPA metabolite levels in the kidney of UUO mice. Data are expressed as means $\pm$ SE (n=5).



### Supplemental Figure 3

**Figure S3.** Arachidonic acid (AA) and eicosapentaenoic acid (EPA) metabolites detected in this study are shown by their metabolic pathways. AA and EPA are metabolized by cytochrome P450, cyclooxygenase (COX) and lipoxygenase (LOX) pathways. (a) Cytochrome P450 converts AA into 11,12-epoxyeicosatrienoic acid (11,12-EET), 5,6-EET and 14,15-EET, and the latter two are hydrolyzed into 5,6-dihydroxyeicosatrienoic acid (5,6-DHET) and 14,15-DHET, respectively. By the COX pathway, AA is converted into prostaglandin E<sub>2</sub> (PGE<sub>2</sub>), PGD<sub>2</sub>, PGF<sub>2 $\alpha$</sub> , PGI<sub>2</sub>, thoromboxane A<sub>2</sub> (TXA<sub>2</sub>) and 12-hydroxyheptadecatrienoic acid (12-HHT). Bioactive PGE<sub>2</sub>, PGD<sub>2</sub>, and PGF<sub>2 $\alpha$</sub>  are converted into inactive forms, 15-keto PGE<sub>2</sub> (15kPGE<sub>2</sub>), 15kPGD<sub>2</sub>, and 15kPGF<sub>2 $\alpha$</sub> , respectively, and further metabolized into 13,14-dihydro-15-keto PGE<sub>2</sub> (dhkPGE<sub>2</sub>), dhkPGD<sub>2</sub>, and dhkPGF<sub>2 $\alpha$</sub> . PGI<sub>2</sub> and TXA<sub>2</sub> are unstable and immediately transformed into 6-keto PGF<sub>1 $\alpha$</sub>  (6kPGF<sub>1 $\alpha$</sub> ) and TXB<sub>2</sub>, respectively, and the former is further metabolized into 6,15-diketo-13,14-dihydro PGF<sub>1 $\alpha$</sub>  (dkdh PGF<sub>1 $\alpha$</sub> ). By the LOX pathway, AA is converted into 5-hydroxyeicosatetraenoic acid (5-HETE), 12-HETE, and 15-HETE, and further metabolized into 5-oxoepoxyeicosatrienoic acid (5-oxoEET), 12-oxoEET, and 15-oxoEET, respectively. Alternatively, 15-HETE is further converted into 5,15-dihydroxyeicosatetraenoic acid (5,15-diHETE) and 8,15-diHETE. (b) Cytochrome P450 converts EPA into 17,18-epoxyeicosatetraenoic acid (17,18-EpETE), 8,9-EpETE, and 18-hydroxyeicosapentaenoic acid (18-HEPE). 17,18-EpETE is hydrolyzed into 17,18-dihydroxyeicosatetraenoic acid (17,18-diHETE) by soluble epoxide hydrolase. Alternatively, COX also converts EPA into 18-HEPE in particular cells. By the COX pathway, EPA is converted into PGE<sub>3</sub>, PGD<sub>3</sub>, PGF<sub>3 $\alpha$</sub> , PGI<sub>3</sub>, and TXA<sub>3</sub>. PGI<sub>3</sub> and TXA<sub>3</sub> are too unstable to detect, and instead we detected their stable metabolites, delta17, 6-keto PGF<sub>1 $\alpha$</sub>  (d17,6kPGF<sub>1 $\alpha$</sub> ) and TXB<sub>3</sub>, respectively. By the LOX pathway, EPA is converted into 5-HEPE, 12-HEPE, and 15-HEPE.



### Supplemental Table 1

The primers used for mRNA detection

Primers	Forward (5'→3')	Reverse (5'→3')
α-SMA (mouse)	AGCCATTTCATTGGGATGG	CCCTGACAGGACGTTGTTA
GAPDH (mouse)	AACTTGGCATTGTGGAAGG	ACACATTGGGGTAGGAACA
Col1a2 (mouse)	CACCCCAGCGAAGAACTCATA	GCCACCATTGATAAGTCTCCCTAAC
Kim-1 (mouse)	TCCACACATGTACCAACATCAA	GTCACAGTGCCATTCCAGTC
α-SMA (rat)	ATCCTGACCCCTGAAGTATCCGAT	CCACGCGAAGCTCGTTATAGA
GAPDH (rat)	ACCATCTTCCAGGAGCGAGA	CCTTCCACGATGCCAAAGTT

**Supplemental Table 2**

The antibody used for Western blotting or immunostaining

Products	Source	Dilution ratio
Rb pAb to alpha smooth muscle actin	Abcam ab569	1:2000
Anti- $\beta$ -actin antibody produced in mouse	Sigma-Aldrich A2228	1:2000
Mouse anti-rabbit IgG-HRP	Santa Cruz sc-2357	1:5000
m-IgG $\kappa$ BP-HRP	Santa Cruz sc-516102	1:5000
Alexa Fluor 647 donkey anti-goat IgG	Invitrogen A-21447	1:200